PECULIARITIES OF THE INFLUENCE OF COMPLEX ALLOYING ON STRUCTURE FORMATION AND MECHANICAL PROPERTIES OF WELDS ON LOW-ALLOYED HIGH-STRENGTH STEELS

V.V. GOLOVKO, V.A. KOSTIN and **G.M. GRIGORENKO**
E.O. Paton Electric Welding Institute, NASU, Kiev, Ukraine

Influence of technological factors (oxygen potential of the flux, welding wire–base metal combination, and cooling rate) on mechanical properties of the studied welds on high-strength low-alloyed 12KhN2MDF and 09G2FB steels was analyzed. Derived results are in agreement with the type of microstructure, composition and distribution of non-metallic inclusions, and features of austenite decomposition in the studied weld metal. It is shown that addition of finely-dispersed refractory inclusions of titanium and zirconium oxides to the weld metal allows achievement of high values of strength (σ_t = = 700–710 MPa) and impact toughness (KCV_{-20} = 80–100 J/cm^2).

Keywords: *arc welding, high-strength low-alloyed steels, ceramic flux, microstructure, austenite decomposition, acicular ferrite, nonmetallic inclusions, mechanical properties*

Continuously growing requirements to metal structures necessitate mastering new steel grades with an increased level of mechanical properties. Alongside low-carbon steels, high-strength low-alloyed (HSLA) steels are ever wider accepted in metallurgical production. Their alloying system envisages an increased content of elements strengthening the solid solution at simultaneous lowering of carbon content [1–3].

The main task in welding HSLA steels is formation of such a microstructure of weld metal, which would ensure both high mechanical properties of the weld proper and equivalent strength of joining of the weld with the base metal. Combination of high values of strength, ducility and toughness can be achieved at formation in weld metal structure of a high content of low-temperature forms of ferrite with fine-grained morphology, namely acicular ferrite (AF) [4, 5].

A rather wide spectrum of microstructures form in weld metal of HSLA steels: AF, polygonal ferrite (PF), Widmanstatten ferrite (WF), ferrite with an ordered (FOS) and disordered (FDS) second phase, as well as microphases (MAC-phase), which form during austenite decomposition. Optimum combination of such strength and ductility properties of weld metal of low-alloyed steels is achieved as a result of a favourable combination of the entire complex of ferrite-cementite structures.

It is known [4, 6] that in this complex AF structure has the highest properties in terms of brittle fracture resistance that is due to its morphological features: AF predominantly forms inside primary crystallites; AF needles have the length of 2–8 μm and thickness of 1–2 μm; their length-width ratio is equal to 1:3–1:10; high-angle boundaries with more than 20° angle of disorientation form between the needles; microphases (carbides or MAC-phase) are observed on the interfaces between the ferrite grains; high dislocation density forms inside AF grains ($\rho = 10^{12}$ cm^{-2}).

AF formation is affected by a whole range of factors, namely: weld metal composition, cooling rate in the temperature range of 800–500 °C, oxygen content in the weld, size of primary austenite grain, composition, size and distribution of nonmetallic inclusions.

At the same time, analysis of published data shows that in a number of cases it is impossible to achieve a high cold resistance of weld metal of HSLA steels, despite the presence of AF structure in them [6, 7]. According to their results, a decrease of impact toughness is possible, despite the presence of a high content of AF in the weld (above 70 %). It should be noted that such a lowering is observed in welds with carbon content of 0.12–0.15 %, that is, possibly, related to the influence of unconsidered structural factor.

In terms of further increase of the values of strength, ductility and impact toughness of the metal of welds and welded joints, bainite structures should form in the weld, preferably, lower bainite. This should be promoted by addition of alloying elements to the melt, which form carbides with melting temperature above that of weld pool metal in the amount that does not exceed their limit solubility in austenite. Such alloying elements as molybdenum, vanadium and niobium satisfy these conditions to the greatest degree.

Niobium dissolved in austenite promotes lowering of A_{c_3} temperature that causes a slowing down of the diffusion processes and promotes formation of rack bainite and martensite structures. Vanadium and molybdenum carbides, while concentrating on the boundary of $\gamma \rightarrow \alpha$ transformation, promote refinement of the forming ferrite grains.

The purpose of this work consisted in selection of metallurgical (oxidizing potential of the flux, flux

Table 1. Composition of base metal and welding wires, wt.%

Steel, wire	C	Mn	Si	S	P	Ti	Ni	Mo	Al	V	Nb	Cu
GNM series												
12KhN2MDF	0.088	0.44	0.253	0.005	0.010	–	2.16	0.27	0.011	0.015	0.005	0.47
Sv-08G1NMA	0.080	1.01	0.050	0.012	0.009	–	1.24	0.25	–	–	–	0.05
GNM-FB series												
09G2FB	0.090	1.70	0.220	0.004	0.008	–	<0.01	0.01	0.035	0.060	0.035	0.01
Sv-10GNMDTA	0.010	1.41	0.220	0.009	0.012	0.08	1.10	0.20	–	–	–	0.45

alloying by refractory element oxides) and technological (combination of base metal and welding wire, cooling rate) factors, ensuring a high level of mechanical properties of welds on HSLA steels.

Investigations envisaged assessment of the influence of weld metal alloying by molybdenum, vanadium and niobium on the structure and properties of weld metal.

To solve the defined task two series of weld metal samples were prepared. Weld metal alloying by molybdenum was performed with welding wires Sv-08G1NMA and Sv-20GNMDTA, and in order to add vanadium and niobium to the weld pool plates of low-alloyed pipe steel 09G2FB were used as base metal.

Chemical composition of base metal and welding wires is given in Table 1. Table 2 gives the results of determination of chemical composition of weld metal obtained in welding with Sv-08G1NMA wire of butt joints of 12KhN2MDF steel (GNM series) and of butt joints produced in welding of 09G2FB steel (GNM-FB series) with Sv-10GNMDTA wire.

Welding was performed using three experimental fluxes with different levels of oxygen potential: acid (flux 13, lg a_O = – 0.83), neutral (9, lg a_O = –1.25) and basic (19, lg a_O = –1.70). Oxygen potential of the flux was calculated by the formula

$$a_O = RTP_{O_2}\ (\text{kJ/mol}),$$

where R is the absolute gas constant, equal to 8.31 J/(mol·K); T is the temperature, K; P_{O_2} is the partial pressure of oxygen over the slag melt.

Slag base of experimental fluxes was based on Al_2O_3–MgO–SiO_2–CaF_2. In order to study the possibilities for controlling the dimensions of ferrite grains in one of the test series (GNM-TiO_2), titanium oxide was added to the flux charge, and in the other (GNM-ZrO_2) it was zirconium oxide.

The following welding modes were used in the experiments: reverse polarity direct current I_w = 700–720 A; U_a = 35–36 V; v_w = 6.9–7.0 mm/s.

Influence of technological factors (oxygen potential of the flux, welding wire–base metal system, cooling rates) on the mechanical properties of the studied welds is shown in Table 3.

Use of welding wire Sv-08G1NMA in welding of 12KhN2MDF steel gives quite low values of yield point (473–500 MPa) and impact toughness, particularly at low testing temperatures of –20 °C (16–20 J/cm^2). Reduction of oxygen potential of the flux (lg a_O: –0.83 → –1.25 → –1.70) practically does not affect these characteristics. Application of Sv-10GNMDTA wire in welding 09G2FB steel leading to weld alloying by vanadium and niobium, increases both the total level of weld metal strength (yield point of 520–545 MPa), and their impact toughness (13–58 J/cm^2). Here, the most favorable is application of a neutral flux with oxygen potential level lg a_O = = –1.25 (weld of GNM09FB series), that allows achieving the level of impact toughness of about 60 J/cm^2 at testing temperature of –20 °C.

The best combination of strength and impact toughness is characteristic of samples of weld metal obtained with a similar combination of welding wire

Table 2. Composition of the metal of studied welds, wt.%

Weld series	C	Mn	Si	S	P	Cr	Ni	Mo	Al	Ti	V	Nb	O
GNM13	0.070	0.51	0.382	0.009	0.012	0.18	1.67	0.26	0.010	0.001	0.005	0.002	0.120
GNM09	0.063	0.53	0.265	0.009	0.013	0.20	1.52	0.25	0.014	0.001	0.007	0.002	0.522
GNM19	0.058	0.58	0.152	0.008	0.013	0.21	1.51	0.25	0.016	0.001	0.009	0.002	0.351
GNM13FB	0.087	1.38	0.453	0.009	0.016	0.08	0.38	0.10	0.021	0.013	0.023	0.013	0.152
GNM09FB	0.081	1.45	0.331	0.004	0.015	0.06	0.39	0.11	0.026	0.017	0.027	0.015	0.035
GNM19FB	0.087	1.59	0.247	0.002	0.015	0.06	0.37	0.12	0.033	0.021	0.040	0.020	0.023
GNM-TiO_2	0.059	1.40	0.533	0.011	0.015	0.25	0.46	0.53	0.019	0.019	0.040	0.006	0.071
GNM-ZrO_2	0.052	1.39	0.499	0.010	0.014	0.24	0.46	0.53	0.020	0.026	0.040	0.006	0.078

Table 3. Mechanical properties of the metal of studied welds (average value from three measurements)

Weld series	$\sigma_{0.2}$, MPa	σ_t, MPa	δ_5, %	ψ, %	*KCV*, J/cm^2, at *T*, °C		
					20	0	−20
GNM13	473.45	617.65	21.50	53.25	38.6	24.3	16.5
GNM09	491.80	603.20	23.50	62.90	48.2	26.7	20.7
GNM19	500.85	620.50	23.25	66.10	48.5	40.4	16.9
GNM13FB	534.15	667.85	26.20	58.85	54.4	35.8	25.9
GNM09FB	545.45	681.55	26.15	68.85	176.8	112.6	58.7
GNM19FB	523.70	688.80	23.85	69.90	45.9	22.6	13.5
GNM-TiO_2	631.45	712.25	26.50	64.95	125.7	99.5	79.5
GNM-ZrO_2	627.85	706.75	25.85	64.00	114.5	109.9	102.8

and base metal, using ceramic flux of basic type with additives of titanium and zirconium oxides (GNM-TiO_2 and GNM-ZrO_2 series), that allowed achieving the yield strength of 700–710 MPa and impact toughness of 80–100 J/cm^2 at testing temperature of −20 °C.

Results of assessment of the influence of cooling rate on the features of austenite decomposition in the metal of the studied welds are given in Figure 1. Investigations conducted in Gleeble 3800 system for simulation of the physical condition of welding showed that at low cooling rates (1 °C/s) of weld metal in the temperature range of 800–500 °C in welds of GNM-FB series austenite decomposition occurs in the region of high transformation temperatures (650–750 °C). With increase of cooling rate (10 °C/s) the region of austenite decomposition shifts into the region of 570–650 °C temperatures. In welds of GNM-TiO_2 and GNM-ZrO_2 series, even at low cooling rates (1 °C/s) austenite decomposition occurs in the region of 550–650 °C (see Figure 1), i.e. in the region of intermediate transformation.

Investigation of the structure and weld metal composition was performed for interpretation of the obtained results. Table 4 gives the quantity of structural constituents in weld metal.

Microstructures of welds of the studied samples are given in Figure 2. Microstructures of welds of GNM series (Figure 2, *a*, *b*), irrespective of the level of oxygen potential in the base metal, consist of coarse-acicular ferrite formations and extended PF precipitates along primary crystallite boundaries.

Microstructure of welds alloyed with molybdenum, vanadium and niobium made using acid flux GNM13FB (Figure 2, *c*) consists of a large quantity (up to 72 %) of classical AF at moderate content of PF and polyherdral ferrite (PHF). Weld made using neutral flux GNM09FB has the highest content of AF (80 %) in the weld metal, and the lowest content of PF, respectively. Microstructure of the series of GNM19FB weld (Table 4) consists of various structural components: AF, PHF, PF, plate-like ferrite (PlF), upper (UB) and lower (LB) bainite, with AF fraction being small (up to 20 %).

Microstructures of welds of GNM-TiO_2 and GNM-ZrO_2 series almost completely consist of finely-dispersed AF, with minimum amount of PF observed (Figure 2, *e*, *f*; Table 4).

In connection with the fact that the weld structure is strongly affected by nonmetallic inclusions, analysis of the composition (Table 5, Figure 3), volume fraction (Table 5) and distribution of nonmetallic inclusions by size (Figure 3) was performed, which showed that with increase of oxidizing potential of the used flux, the volume fraction of nonmetallic inclusions in the weld metal increases (Table 5), while inclusion size decreases to 0.3–0.5 μm (Figure 3, *c*, *d*).

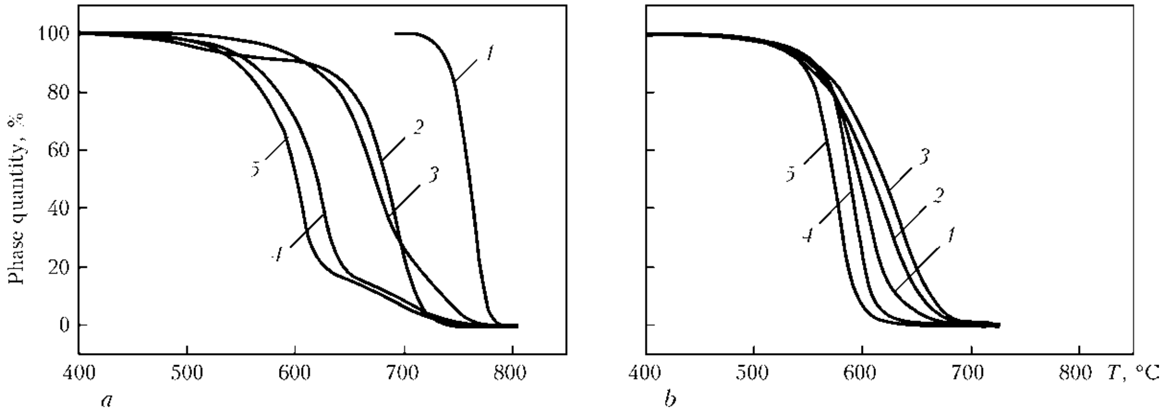

Figure 1. Influence of cooling rate of 1 (*a*) and 10 (*b*) °C/s on the nature of austenite decomposition in the studied welds: *1* — GNM09FB; *2* — GNM19FB; *3* — GNM13FB, *4* — GNM-ZrO_2; *5* — GNM-TiO_2

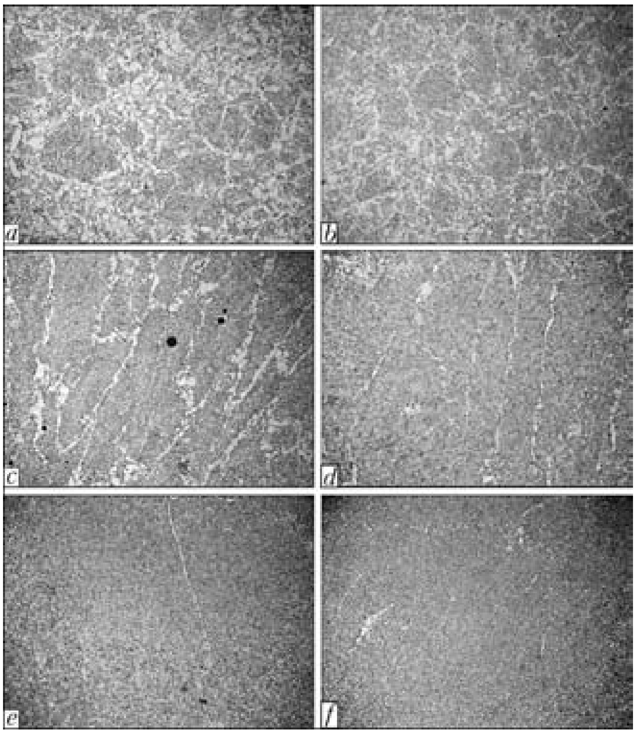

Figure 2. Microstructures (×200) in the center of sample weld: *a* — GNM13; *b* — GNM19; *c* — GNM13FB; *d* — GNM19FB; *e* — GNM-TiO_2; *f* — GNM-ZrO_2

Analysis of the results of mechanical testing of studied weld metal showed the non-rationality of application of Sv-08G1NMA welding wire in welding of 12KhN2MDF steel, as irrespective of the level of flux oxygen potential rather low values of yield point (473–500 MPa) and impact toughness are achieved, particularly at low testing temperatures of −20 °C (16–20 J/cm^2). Analysis of the conducted metallographic investigations showed that this is related primarily to formation of coarse-acicular ferrite and large amount of PF along the boundaries of primary crystallites (see Figure 2, *a*, *b*). This is due to considerable content in the metal of welds of this series (GNM, see Table 2) of nickel (1.5–1.6 %), molybdenum (0.25–0.26 %) at insignificant content of titanium (0.001 %), vanadium (0.005–0.009 %) and niobium (0.002 %). Thus, metal of the studied welds turned out to be «over-alloyed» by nickel and molybdenum. The forming coarse (more than 1.5 μm) nonmetallic inclusions also had a negative influence.

Table 4. Quantity of structural components in the studied welds, %

Weld series	AF	PHF	PF	PlF	LB	UB	Austenite grain size, μm
GNM13FB	72	17	11	–	–	–	400
GNM09FB	80	9	11	–	–	–	350
GNM19FB	20	18	10	7	6	24	300
GNM-TiO_2	95	3	2	–	–	–	50
GNM-ZrO_2	97	1	2	–	–	–	50

A more favorable combination is that of 09G2FB steel and Sv-10GNMDTA wire. Application of Sv-10GNMDTA welding wire in welding of 09G2FB steel leads to the level of nickel (0.37–0.39 %) and molybdenum (~0.1%) content in the weld metal turnig out to be much lower than in the previous combination of materials (see Table 2). Moreover, weld metal alloying by titanium (0.01–0.02 %), vanadium (0.02–0.04 %) and niobium (0.01–0.02 %) increases that results in an increase of both the total level of weld metal strength (yield point of 530–545 MPa), and their impact toughness (13–58 J/cm^2). The best values of mechanical properties were achieved at application of neutral flux (lg $a_O = -1.25$, GNM09FB weld series), which allowed achieving the level of about 60 J/cm^2 at testing temperature of −20 °C.

Obtained results found an explanation during analysis of microstructure of metal of GNM-FB series welds.

Analysis of the structural condition of the studied welds showed that the high contamination of GNM13FB weld (acid flux) by nonmetallic inclusions of more than 1 μm size promotes formation of solid precipitates (fringes) of PF along the grain boundaries.

Microstructure of the weld of GNM09FB series consists of finely-dispersed AF (~80 %) and small amount of PF, which is what ensures the high mechanical properties of the weld. Optimum content of dispersed titanium carbides (6.86 %) and fine inclusions of oxide type (9.68 %, see Table 5) in the microstructure allowed ensuring a fabourable combination of the values of strength, ductility and toughness

Table 5. Composition, total fraction of nonmetallic inclusions, V_{NMI}, fraction of finely-dispersed inclusions ($V_{<0.3}$) in the metal of studied welds

Weld series	Elemental content in inclusions, wt.%						V_{NMI}, %	$V_{<0.3}$, %
	O	Al	Si	S	Ti	Mn		
GNM13FB	25.05	5.27	15.56	1.86	3.57	48.69	0.86	11.40
GNM09FB	38.74	24.09	3.17	1.07	6.86	26.07	0.21	9.68
GNM19FB	43.81	29.39	1.08	0.79	5.82	19.12	0.10	21.56
GNM-TiO_2	28.44	6.62	13.56	3.34	5.47	42.56	0.33	80.34
GNM-ZrO_2	35.05	6.61	8.15	1.83	13.05	35.30	0.47	85.72

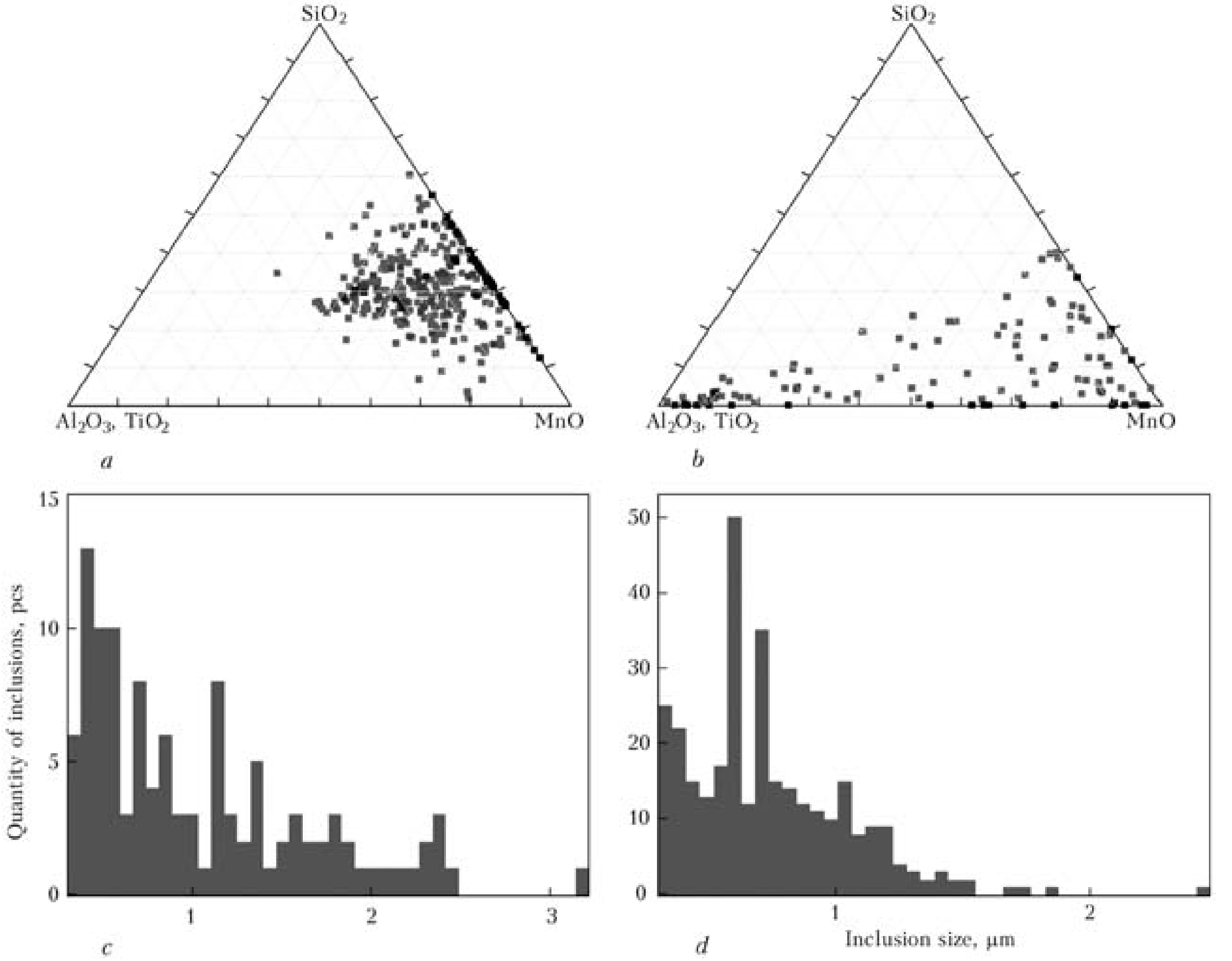

Figure 3. Nature of distribution of nonmetallic inclusions by composition (*a*, *b*) and dimensions (*c*, *d*) in GNM-TiO_2 (*a*, *c*) and GNM09FB (*b*, *d*) welds

in the metal of GNM09FB series weld, produced when welding with neutral flux (see Table 3). Here, not the dispersion, but grain boundary strengthening started having the leading role in ferrite matrix strengthening, its distinctive feature being its positive influence on increase of both the values of strength and toughness of the metal.

At formation of mechanical properties of metal in the structure of GNM19FB series weld the contribution of dispersion strengthening turned out to be too high, which is caused by a high content of finely-dispersed (< 0.3 μm, see Table 5) inclusions in the weld structure. X-ray spectral analysis of these inclusions showed that they contain a considerable amount of chromium carbides and titanium carbonitrides, which promotes formation of plate-like forms of ferrite, as well as UB, characterized by higher hardness.

Lowering of the temperature of the end of bainite transformation, formation of carbide-free bainite, combination of the content of oxide nonmetallic inclusions of up to 1.0 μm size and dispersed carbides of up to 0.3 μm size, which was ensured by the appropriate level of oxygen potential of flux 9 ($\lg a_O = -1.25$), promoted formation of a large amount of AF in GNM09FB weld metal. As a result, the level of impact toughness of weld metal increased in the entire temperature range of testing (see Table 3).

Analysis of mechanical properties of welds of GNM-FB series showed that although the level of strength and ductility increased somewhat (see Table 3), compared to welds of GNM series, impact toughness values still remain on a rather low level, particularly in the field of negative temperatures. All that necessitated a search for new combinations of welding wire compositions and types of welding fluxes, in order to simultaneously ensure high values of strength, ductility and impact toughness by redistribution of alloying elements (nickel, molybdenum, titanium, vanadium and niobium) between the base metal, welding wire and flux.

In this connection, two more welds were made in the same system of base metal–welding wire. Proceeding from analysis of agglomerated fluxes currently applied in pipe-welding plants of the countries of the European Union, Russian Federation and Ukraine, their welding was performed using test flux of aluminate-basic type (($CaO + MgO$) %, ($Al_2O_3 + MnO$) %, SiO_2 %, CaF_2 %). In one of the variants titanium oxide was added to the flux charge (weld of GNM-TiO_2), in another variant it was zirconium oxide (weld

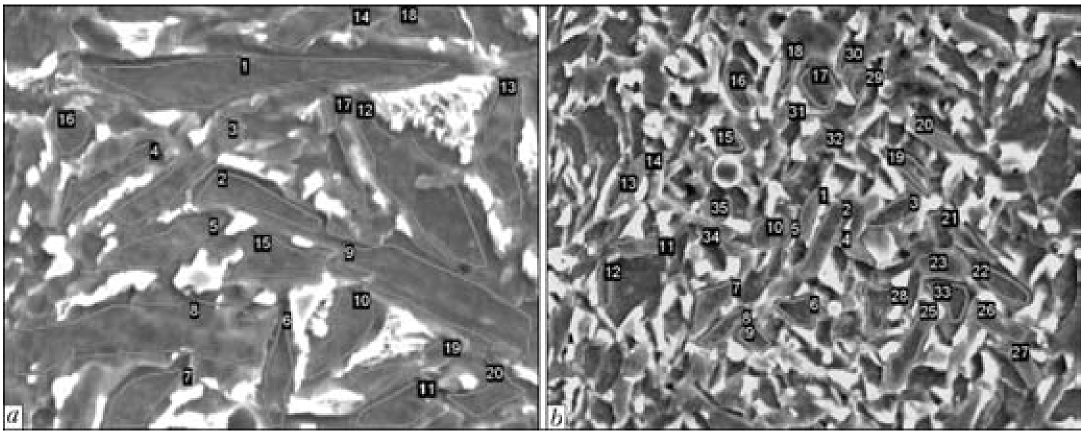

Figure 4. Comparison of AF morphology (×2000) in welds of GNM19FB (*a*) and GNM-TiO_2 (*b*) series (numbers show microanalysis regions)

of GNM-ZrO_2 series) in order to study the possibilities of improvement of mechanical properties of the weld through control of the kinetics of ferrite grain growth.

Analysis of mechanical properties of welds made with additives of titanium and zirconium oxides (see Table 3) showed that addition of TiO_2 and ZrO_2 refractory oxides to the weld pool allowed increasing the ultimate strength up to 700–710 MPa and impact toughness up to 80–102 J/cm^2 at the test temperature of −20 °C.

It was possible to interpret the obtained results when studying their microstructure. Analysis of the structural state of welds of GNM-TiO_2 and GNM-ZrO_2 series showed that the welds developed an almost completely (95 %) AF structure (see Table 4 and Figure 2, *e*, *f*).

Change of the temperatures of phase transformations during austenite decomposition in GNM-TiO_2 and GNM-ZrO_2 welds, compared to welds of GNM-FB series, was manifested in the principal difference in the type of AF formed in these welds (Figure 4).

AF forming in the weld of GNM-TiO_2 series is much finer (up to 1 μm) than in the weld of GNM19FB series (5–10 μm) with more chaotically located needles. This is obviously related to the influence of both primary titanium and zirconium oxides, and the possibility of initiation of ferrite needles on the secondary oxides precipitating from the melt. MAC-phase forming between the needles is finer, and has a smoothed shape (without sharp angles) and is uniformly distributed. Analysis of the content of alloying elements showed a lower content of manganese and silicon and higher content of titanium and carbon in the ferrite needles.

Addition of TiO_2 and ZrO_2 to the flux charge leads to a considerable increase of the quantity of nonmetallic inclusions of not less than 1 μm size, compared to welds of GNM-FB series (see Figure 5, *b*, *c* and Table 5) promoting AF formation [8].

Analysis of the influence of complex alloying of weld metal on the kinetics of austenite decomposition (see Figure 1) showed an essential difference made by finely-dispersed inclusions of titanium and zirconium oxides in this process. A very gently sloping part of the curve of austenite decomposition in the temperature range of 750–650 °C indicates that in these welds austenite decomposition in the region of diffusion-induced ferrite transformation practically does not take place, whereas the main part of decomposition occurs at temperatures of 600–500 °C, i.e. in the region of low-temperature bainite (intermediate) transformation.

Increase of the cooling rate in the temperature range of 800–500 °C from 1 up to 10 °C/s, shifts austenite decomposition temperature into the region of lower temperatures, leveling off the differences in the nature of decomposition for all the studied welds (see Figure 1).

Complex alloying of weld metal by elements stabilizing the austenitic phase (manganese, nickel, molybdenum), as well as vanadium and titanium, which form carbides unstable at high temperatures, leads to formation of coarse (300–400 μm) primary austenite grains and formation of secondary structure with in-

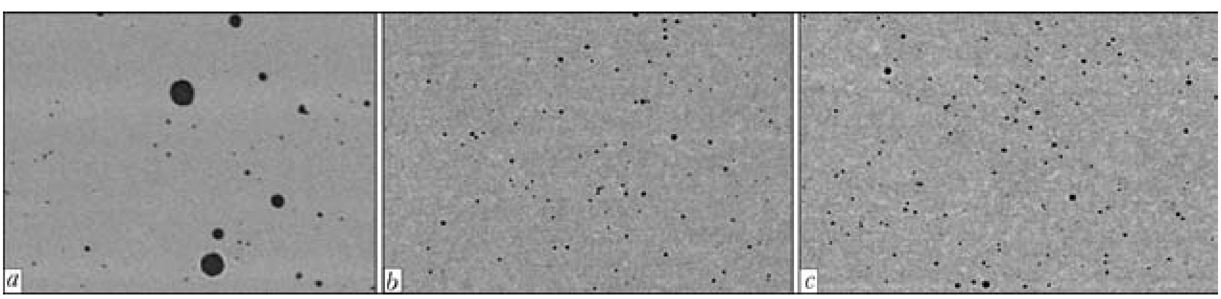

Figure 5. Microstructures (×1000) of nonmetallic inclusions in studied welds of GNM13FB (*a*), GNM-TiO_2 (*b*), GNM-ZrO_2 (*c*) series

creased content of brittle structural components. Addition of finely dispersed refractory inclusions of titanium and zirconium oxides to the weld metal allowed a considerable reduction of the size of primary austenite grain (to 50 μm) and shifting the transformation region into the low temperature zone, thus promoting formation of AF (up to 95–97 %). In this case weld metal has an optimum combination of the values of strength, ductility and toughness to the level corresponding to the requirements made of metal of welds of strength grade K65 ($\sigma_{0.2}$ > 570 MPa, σ_t > > 620–700 MPa, KCV_{-20} > 98 J/cm^2 according to specification of Khartsyzsk Pipe Plant) and higher.

Thus, in order to ensure a combination of high values of strength, ductility and impact toughness, secondary microstructure of the metal of welds of the studied alloying system should form in the low-temperature region of bainite transformations and should contain more than 50 % of structural components of higher toughness (carbide-free bainite, AF). Size of ferrite grains of such a structure should not be higher than 100 μm (up to 50 μm is optimal). To achieve a fine-grained structure it is necessary to add niobium and vanadium to the weld metal and ensure their carbide formation. Complex alloying of the weld (nickel, molybdenum, titanium, vanadium and niobium) is limited to the requirement, in keeping with which solid-solution strengthening of the structure should be lower than grain-boundary and dispersion strengthening. Parameters of welding consumables should ensure formation of finely-dispersed nonmetallic inclusions and carbides (carbonitrides) of alloying elements (titanium, vanadium, molybdenum) in the weld metal.

CONCLUSIONS

1. Investigations confirmed the advantages of application of agglomerated (ceramic) fluxes in welding HSLA steels. Ceramic fluxes of aluminate-basic type should be used to improve the mechanical properties of the metal of welds of HSLA steels that will allow simultaneous improvement of strength, ductility and impact toughness of weld metal.

2. It is not rational to use Sv-08G1NMA welding wire in welding of 12KhN2MDF steel, as the achieved strength (σ_t = 473–500 MPa) and impact toughness (KCV_{-20} = 16–20 J/cm^2) values are rather low, irrespective of the level of flux oxygen potential.

3. To ensure high mechanical properties in welding 09G2FB steel with Sv-10GNMDTA welding wire, it is rational to use neutral flux with the level of oxygen potential lg a_O = –1.25. Complex alloying of weld metal allows achieving high values of strength (σ_t = = 680 MPa) and impact toughness (KCV_{-20} = = 58 J/cm^2).

4. Oxygen potential and complex alloying ability of welding consumables should be selected so as to ensure formation of nonmetallic inclusions consisting predominantly of dispersed oxides (of up to 1.5 μm size) and finely-dispersed carbides and carbonitrides (of up to 0.3 μm size) in the weld metal. Composition and volume fraction of the oxide phase determine the conditions of formation of AF structure, carbides and carbonitirdes control formation of bainite structures.

5. Addition of finely-dispersed refractory inclusions of the type of titanium and zirconium oxides to the weld metal allows a considerable lowering of the size of primary austenite grain (to 50 μm) and shifting the transformation region into that of low temperatures, promoting formation of a completely acicular structure (up to 95–97 %). High values of strength (σ_t = 700–710 MPa) and impact toughness (KCV_{-20} = = 80–100 J/cm^2) are achieved as a result of complex alloying of weld metal and adding titanium and zirconium oxides to the metal.

1. Goldshtejn, M.I., Farber, V.M. (1979) *Dispersion strengthening of steel*. Moscow: Metallurgiya.
2. Lagneborg, R., Sivetsky, T., Zayats, S. et al. (2001) *Role of vanadium in microalloy steels*. Ekaterinburg: Mariya.
3. Khajsterkami, F., Khulka, K., Matrosov, Yu.I. et al. (1999) *Niobium-containing low-alloy steels*. Moscow: Intermet Engineering.
4. Pokhodnya, I.K., Golovko, V.V., Denisenko, A.V. et al. (1999) Effect of oxygen on formation of acicular ferrite structure in low-alloy metal of welds. *Avtomatich. Svarka*, **2**, 2–10.
5. Ito, G., Nakanishi, M. Study on Charpy impact properties of weld metals with submerged arc welding. *IIW Doc. XI-A-113–75*.
6. Svensson, L.-E., Gretoft, B. (1990) Microstructure and impact toughness of C–Mn weld metals. *Welding Res. Supp.*, Dec., 454–461.
7. Evans, G.M. The effect of carbon on the microstructure and properties of C–Mn all-weld-metal deposits. *IIW Doc. II-A-546–81*.
8. Cole, W., Colvin, P. (1971) Submerged arc welding of higher tensile steels. *Metal Constr. and British Welding J.*, **3**, 131–135.